Impairment of renal steroidogenesis at the onset of diabetes

Melina A. Pagotto, María L. Roldán, Sara M. Molinas, Trinidad Raices, Gerardo B. Pisani, Omar P. Pignataro, Liliana A. Monasterolo

PII: S0303-7207(21)00014-9

DOI: https://doi.org/10.1016/j.mce.2021.111170

Reference: MCE 111170

To appear in: *Molecular and Cellular Endocrinology*

Received Date: 23 September 2020

Revised Date: 13 December 2020

Accepted Date: 11 January 2021

Please cite this article as: Pagotto, M.A., Roldán, M.L., Molinas, S.M., Raices, T., Pisani, G.B., Pignataro, O.P., Monasterolo, L.A., Impairment of renal steroidogenesis at the onset of diabetes, *Molecular and Cellular Endocrinology*, https://doi.org/10.1016/j.mce.2021.111170.

CRediT author statement:

Melina A. Pagotto: Conceptualization, Investigation, Writing- Original draft preparation. **María L. Roldán:** Investigation. **Sara M. Molinas:** Investigation, Writing - Review & Editing. **Trinidad Raices:** Investigation, Writing - Review & Editing. **Gerardo B. Pisani:** Investigation. **Omar P. Pignataro:** Conceptualization, Supervision. **Liliana A. Monasterolo:** Conceptualization, Writing- Original draft preparation, Funding acquisition, Supervision.

Impairment of renal steroidogenesis at the onset of diabetes

Melina A. Pagotto[a], María L. Roldán[b], Sara M. Molinas[b,c], Trinidad Raices[d], Gerardo B. Pisani[e], Omar P. Pignataro[d,f], Liliana A. Monasterolo[b,c,g] *

[a]Institute of Experimental Physiology, National Scientific and Technical Research Council (IFISE-CONICET), Suipacha 531, PC 2000, Rosario, Argentina. melina.pagotto@gmail.com
[b]L, Suipacha 531, PC 2000, Rosario, Argentina. roldan.casoli@gmail.com
[c]National Scientific and Technical Research Council (CONICET).
sara_molinas@yahoo.com.ar
[d]Laboratory of Molecular Endocrinology and Signal Transduction, Institute of Biology and Experimental Medicine (IBYME)- National Scientific and Technical Research Council (CONICET), PC C1428ADN, Buenos Aires, Argentina. triniraices@hotmail.com
[e]Morphology, Faculty of Biochemical and Pharmaceutical Sciences, National University of Rosario, Suipacha 531, PC 2000, Rosario, Argentina. gerpisani@yahoo.com.ar
[f]Department of Biological Chemistry, School of Sciences, University of Buenos Aires (UBA), PC 1428 Buenos Aires, Argentina. oppignataro@gmail.com
[g]Research Council of the National University of Rosario (CIC-UNR)
lmonaste@fbioyf.unr.edu.ar

*Cooresponding author: Liliana A. Monasterolo. Pharmacology, Faculty of Biochemical and Pharmaceutical Sciences, National University of Rosario, Suipacha 531, PC 2000, Rosario, Argentina. l_monasterolo@yahoo.com; lmonaste@fbioyf.unr.edu.ar

Abstract

Accumulating evidence indicates the association between changes in circulating sex steroid hormone levels and the development of diabetic nephropathy. However, the renal synthesis of steroid hormones during diabetes is essentially unknown. Male Wistar rats were injected with streptozotocin (STZ) or vehicle. After one week, no changes in functional or structural parameters related to kidney damage were observed in STZ group; however, a higher renal expression of proinflammatory cytokines and HSP70 was found. Expression of Steroidogenic Acute Regulatory protein (StAR) and P450scc (CYP11A1) was decreased in STZ kidneys. Incubation of isolated mitochondria with 22R-hydroxycholesterol revealed a marked inhibition in CYP11A1 function at the medullary level in STZ group. The inhibition

of these first steps of renal steroidogenesis in early STZ-induced diabetes led to a decreased local synthesis of pregnenolone and progesterone. These findings stimulate investigation of the probable role of nephrosteroids in kidney damage associated with diabetes.

Keywords: kidney; steroidogenesis; diabetes; CYP11A1; StAR; pregnenolone

Abbreviations: 3β-HSD, 3β-hydroxysteroid dehydrogenase; CX, renal cortex; CYP11A1 P450, side chain cleavage enzyme; DN, diabetic nephropathy; FEglucose, fractional excretion of glucose; FEH_2O, fractional excretion of water; $FENa^+$, fractional excretion of sodium; GFR, Glomerular filtration rate; HSP70, heat shock protein 70; IL-1β, interleukin-1β; IL-6, interleukin-6; IMM, inner mitochondrial membrane; M, renal medulla; MPO, myeloperoxidase; P4, progesterone; P5, Pregnenolone; RIA, radioimmunoassay; StAR, Steroidogenic Acute Regulatory protein; STZ, streptozotocin; T, testosterone; TGF-β, transforming growth factor β; TSPO, 18 kDa Translocator Protein; UFR, urine flow rate

1. Introduction

Despite novel therapies and approaches, nephropathy is still a leading cause of mortality in diabetic patients. The development of diabetic nephropathy (DN) is a slow process that usually becomes clinically evident after several years and continues with a progressive deterioration of kidney function. Signs of renal damage include microalbuminuria and decreased glomerular filtration rate (GFR) (Sulaiman, 2019). The alterations in the renal structure that characterize DN are associated with proinflammatory and profibrotic phenomena. Transforming growth factor β (TGF-β) plays a fundamental role in the hypertrophic process and in the profibrotic manifestations, including glomerulosclerosis and interstitial fibrosis (Ziyadeh, 2004). The inflammatory process generates a stress environment, which could induce the expression of heat shock protein 70 (HSP70) to counteract the deleterious effect of pro-inflammatory cytokines (Chebotareva et al., 2017). The major goal of basic research related to DN is to expand the knowledge of the mechanisms responsible for the onset and progression of the disease. There is an urgent need to detect early mediators of kidney damage that are useful as predictors and / or therapeutic targets in DN.

Accumulated evidence points toward a strong association between changes in circulating sex hormone levels and kidney disease in diabetic patients (Maric, 2009, Wang et al., 2019). In animal models of diabetes, it was observed that renal deterioration coincides with alterations

in the plasma levels of steroid hormones, such as testosterone, estradiol or progesterone, and the restoration of the levels of these hormones induces an improvement in kidney damage. (Xu et al., 2008 and 2009; Prabhu et al., 2010; Manigrasso et al., 2011; Al-trad et al., 2015). This information strongly supports the relevance of steroid hormones in the pathophysiology of diabetic kidney disease.

The effects of steroid hormones on the kidney may depend on the levels of circulating hormones and on the synthesis and / or metabolism of hormones in the kidney tissue itself. The adult rat kidney is capable of metabolizing steroid hormones (Dalla Valle et a., 1992 and 2004) and we previously reported that it also synthesizes pregnenolone, the precursor of all steroids (Pagotto et al., 2011). Therefore, the kidney can be considered as an extra-glandular steroidogenic organ, and the steroids that are locally synthesized / metabolized might act as paracrine or autocrine factors playing a role in the maintenance of renal physiological functions and/or in the progression of pathological situations (Dalla Valle et al., 2004; Pagotto et al., 2011). This point of view encourages the investigation of the renal steroidogenic capacity in an experimental model of diabetes.

The first step in the steroid biosynthesis pathway is the translocation of cholesterol from outer to inner mitochondrial membrane, where cytochrome P450 side chain cleavage enzyme (CYP11A1) catalyzes its cleavage to pregnenolone (Farkash et al., 1986). Cholesterol delivery from outer to inner mitochondrial membrane is promoted by Steroidogenic Acute Regulatory protein (StAR) (Krueger and Orme-Johnson, 1983, Lin et al., 1995). For a long time, the 18 kDa Translocator Protein (TSPO) was believed to be another requirement for regulating cholesterol transport and a series of experiments demonstrated its association with StAR in cholesterol transfer (Krueger and Papadopoulos, 1990, Papadopoulos and Miller, 2012). However, this evidence accumulated over decades has been recently challenged by experiments indicating that TSPO would not be essential for steroid biosynthesis; thus, the role of TSPO remains uncertain (Stocco et al., 2017). Therefore, the first steps of the renal steroidogenic pathway, which determine the *de novo* synthesis of pregnenolone and the consequent production of other nephrosteroids, basically depend on the proteins: StAR, CYP11A1 and, probably, TSPO.

The main objective of this work was to investigate the effects of short-term diabetes, prior to the onset of kidney injury, on renal expression of proteins involved in steroidogenesis and on the local synthesis of pregnenolone. Indicators of inflammatory and profibrotic processes and HSP70 expression in kidney tissue were also evaluated.

2. Materials and methods

2.1.Animals and treatments

Adult male Wistar rats (3 months, 300-350 g body weight) were used in this study. All animal procedures were conducted in accordance with the Guide for the Care and Use of Laboratory Animals (8th ed., 2011, published by The National Academies Press, US) and approved by our Institutional Animal Care and Use Committee.

Diabetes was induced by a single intravenous injection of 50mg/kg b.w. streptozotocin (STZ; ICN, cat# 100775) dissolved in a citrate buffer solution (0.1M citric acid, 0.1M sodium citrate pH 4.50). Age matched controls (C) received only the vehicle. After five days, the animals were placed in individual metabolic cages for two days for acclimation as previously described by our group (Brovedan et al., 2017). The following day, one week after the STZ or vehicle injection, urine was collected over a period of 16 hours (6:00 p.m. to 10:00 a.m.). At the end of this period, rats were anesthetized with sodium thiopental (70 mg/kg b.w., i.p.). Blood was collected from inferior cava vein and kidneys were removed for further experiments. Tissue from cortex (CX) and medulla (M) was separated as required. Blood was centrifuged and serum was separated for the measurement of progesterone (P4), testosterone (T) and for biochemical determinations. Urine volume was recorded and urinary albumin, creatinine, glucose and sodium were determined.

2.2.Histopathological studies

According to the standard procedure, the kidneys were prepared for observation by light microscopy. The tissue was fixed in 10% formaldehyde, embedded in paraffin, and sectioned (5 µm). The sections were stained with haematoxylin and eosin (H&E) or periodic acid – Schiff (PAS) or Masson's trichrome or Direct Red 80/picric acid and examined under a light microscope.

2.3.Myeloperoxidase activity

MPO activity was measured in total homogenates as previously described (Pompermayer et al. 2005). To verify MPO heat resistance, the tubes were incubated in a water bath for 2 h at 60 °C (Schierwagen et al. 1990) and then centrifuged for 15 min at 10 000g at 4 °C. MPO activity was measured by verifying the change in optical density (OD) at 652 nm in the presence of 1.6 mM tetramethylbenzidine and 0.5 mM H2O2 in 80 mM Na_3PO_4 (pH = 5.40). Results were expressed as relative units of MPO / g of wet tissue, with one unit of MPO being the amount of enzyme that breaks down 1 µM H2O2 / min at 25 ° C.

2.4.Isolation of Mitochondria

Fragments of CX and M tissue from C and STZ groups were homogenized (1 g of tissue per 5 ml of buffer) in isolation buffer (IB) containing sucrose 0.27 M, EDTA 1 mM, Tris-HCl 5 mM and a mixture of protease inhibitors (phenylmethysulfonyl fluoride 1 mM, leupeptin 1 mM), pH 7.40. Homogenates were centrifuged at 500 g for 10 min at 4ºC. The resulting supernatant (total homogenate, H) was centrifuged at 5,500 g for 15 min at 4 ºC. The pellet, consisting of mitochondrial fraction (MIT) was then resuspended in 800 µl of IB for isolation of mitochondrial membranes or in reaction buffer for pregnenolone synthesis as described in *2.9.*.

2.5.Isolation of inner mitochondrial membranes

The preparation of the inner mitochondrial membrane (IMM) was carried out by adding digitonin to the MIT suspension of CX and M tissue as previously performed in our laboratory (Pagotto et al., 2011), following the technique described by Calamita et al. (2005). The enrichment in IMM was confirmed by immunoblotting using an antibody against prohibitin, a protein that is abundantly expressed in IMM (Nijtmans et al., 2000).

2.6.Reverse transcription polymerase chain reaction

IL-1β, IL-6, TGF- β, TSPO and StAR mRNA levels in cortical and medullary samples were measured by reverse transcription polymerase chain reaction (RT-PCR) as previously described (Pagotto et al., 2011). Total RNA was extracted using the Trizol Reagent method (Invitrogen, Life Technologies) according to manufacturer's instructions. The synthesis of cDNA by oligo dT-primed reverse transcription was performed using the Mooney Murine Leukaemia Virus Reverse Transcriptase (M-MLV RT) (Invitrogen, Life Technologies). The primers and Tm used were: IL-1β: Tm 58°C, product length: 184 bp, forward 5'-CTGACAGACCCCAAAAGATT-3', reverse 5´-AGAAGGTGCTCATGTCCTCA-3'; IL-6: Tm 65°C, product length: 154 bp, forward 5´-TGGAGTCACAGAAGGAGTGGCTAAG-3', reverse 5´-TCTGACCACAGTGAGGAATGTCCAC-3'; TGF-β1: Tm 54°C, product length: 293 bp; forward 5´-GACTACTACGCCAAAGAAG-3', reverse 5´-TCAAAAGACAGCCACTCAGG-3'; TSPO: Tm 58 ºC, product length: 234 bp, forward 5´-GTACAACTGTCCCCGCATG, reverse 5' CCATGCTCAACTACTATGTATGGC-3´; StAR: Tm 57 ºC, product length: 746 bp, forward 5'- TACTACCCCTCTCGTTGTCCT-3', reverse 5'-CCAGGAGCTGTCCTACATCCAG-3' ; GAPDH: product length: 452 bp, forward 5'-TCCACCACCCTGTTGCTGTA-3', reverse 5'-ACCACAGTCCATGCCATCAC-3'; β-Actina: product length: 911bp, forward 5´-GGTGACGAGGCCCAGAGCAAG-3', reverse 5´- GATCCACATCTGCTGGAAGGT-3' .

Amplified PCR products were electrophoresed in 1.2% agarose gels, stained with ethidium bromide, and analysed using a Kodak Electrophoresis Documentation Analysis System. The intensity of bands was measured by densitometry for semiquantitation.

2.7.Immunoblotting Analysis

Samples were run on sodium dodecyl sulphate 8-12 % polyacrylamide gels (SDS-PAGE) (Bio-Rad Mini Protean 3, Hercules, CA, USA) as previously described (Pagotto et al., 2011). The detection of StAR was carried out in MIT samples, the detection of CYP in IMM samples and the detection of HSP70, TSPO or IL-1β in total homogenate samples. Separated proteins were transferred onto nitrocellulose membranes (BioRad). Membranes were then incubated overnight with the corresponding primary antibody against: StAR (gift from Dr. Walter L. Miller, University of California, San Francisco), CYP11A1 (gift from Dr. Dale B. Hales, Southern Illinois University, Carbondale), TSPO (Santa Cruz Biotechnology), IL-1β (Abcam), HSP70 (Santa Cruz Biotechnology). After washing, membranes were incubated with HRP-conjugated anti-rabbit antibody (Amersham Bioscience) or with HRP-conjugated anti-goat antibody (Santa Cruz Biotechnology). The membranes were developed with luminal-chemiluminescent substrate (ECLPlus, Amersham Bioscience), according to the manufacturer´s protocols. To verify the protein loading in MIT and IMM samples, membranes were incubated with an anti-prohibitin antibody (Abcam). Prohibitin is an abundant chaperone protein localized in the IMM (Nijtmans et al., 2000); and we have previously used it as IMM marker and as a loading control in mitochondrial and IMM fraction samples (Pagotto et al., 2011). An anti-β-actin antibody (Santa Cruz Biotechnology) was used as loading control in total homogenate samples. Then, membranes were revealed as described above. Densitometric analysis of the Western blot bands intensity was performed.

2.8.StAR and CYP11A1 Immunohistochemistry

Kidney slices from C and STZ group were fixed in 10 % v/v phosphate buffer (PB)-formalin solution pH 7.40 and embedded in low melting point paraffin. Briefly, 5 µm paraffin sections were deparaffinized in xylene. After hydration, antigen retrieval was carried out by microwaving sections twice in 10 mM citrate buffer pH 6.0 for 5 min. Sections were placed in 3 % hydrogen peroxide in PB for 15 min to inhibit the endogenous peroxidase activity, and placed for 1 h at room temperature in 1 % bovine serum albumin in PB containing 0.1 % Triton X-100 to block nonspecific binding sites and to improve antibody penetration. After incubation with a polyclonal antibody against StAR (1:70 dilution) or CYP11A1 (1:150 dilution) at 4 ºC for 24 h, sections were washed three times with PB for 5 min. Tissue

samples were subsequently incubated with biotynilated goat anti-rabbit immunoglobulin for 15 min, and then, incubated with streptavidin-HRP (UtraMarque^{TM} HRP Detection System) for 15 min. Immunoreactivity was detected with 2.7 mM 3,3'-diaminobenzidine tetrahydrochloride in PB with 0.03 % hydrogen peroxide w/v. The reaction was stopped by adding distilled water. Sections were lightly counterstained with hematoxylin, dehydrated, cleared and finally mounted. As a negative control, the primary antibody was replaced with normal rabbit serum in PB. Slices of rat adrenal gland were processed in the same way and used as positive controls.

2.9. Pregnenolone and Progesterone Synthesis

Pregnenolone (P5) and P4 synthesis protocol was previously used in our laboratory (Pagotto et al., 2011). The technique used was modified from others described by other authors (Espinosa-Garcia et al., 2000; Esparza-Perusquía, 2015). Briefly, transformation of cholesterol into P5 and P4 was measured in reaction buffer containing 250 mM sucrose, 5 mM $MgSO_4$, 20 mM KH_2PO_4, 25 mM Tris-HCl, 0.2 mM EDTA, 1mg/ml bovine albumin, 20 mM glucose-6-phosphate, 2 U glucose-6-phosphate dehydrogenase and in the absence or in the presence of 50 µM 22R-hydroxycholesterol (22R-OHC), a membrane-permeant cholesterol analogue. MIT suspensions were incubated at 37 ºC for 5 minutes in a shaking bath. The reaction was started by the addition of 5 mM sodium isocitrate, 0.5 mM $NADP^+$ and 0.5 mM NADPH (final volume 50 µl for medullary mitochondria and 100 µl for cortex mitochondria). After 45 min, the reaction was stopped with methanol. After methanol was evaporated, the samples were used to determine the P5 and P4 concentration by RIA.

2.10. RIA measurements

Tissue P4 and T extraction was performed as previously described (Pagotto et al., 2011). The preparation of samples for the measurement of P4 and P5 in mitochondria was explained in Section *2.9.* Serum P4 and T were determined after two extractions with 5 ml ethyl ether (Merck). All the evaporated residues obtained were resuspended in RIA buffer (Na2HPO4 40 mM, NaH2PO4 30 mM, NaCl 150 mM, sodium azide 0.01%, gelatine 0.1%, pH 7.0) and appropriate aliquots were assayed for P5, P4 and T by RIA, as previously described (Del Punta *et al.*, 1996). The intraassay and interassay variations were 7.5 and 15.1% for P5, 8.0% and 14.2% for P4 and 7.3% and 13.2% for T, respectively. RIAs were performed using ^{3}HPregnenolone (50.5 Ci mmol^{-1}), ^{3}HProgesterone (80.2 Ci mmol^{-1}) and ^{3}HTestosterone (80 Ci mmol^{-1}) (Amersham International, Buckinghamshire, GB). A volume of 100 µl of each sample was incubated for 16 h at 4 ºC with 100 µl of ^{3}HP4 or ^{3}HT or ^{3}HP5 and 100 µl of the dilute corresponding antibody. After the incubation, the free hormone was separated from the

complex hormone-antibody using a carbon suspension Norit A 0.5 % w/v-dextran 70 0.05 % w/v in RIA buffer and then centrifuged at 1,400 g for 10 min. The supernatants were transferred to counting vials containing 2.5 ml of scintillation liquid Hisafe 3. The radioactivity was measured with Perkin Elmer 2800 TR Liquid Scintillation Counter. The utility range of the assay was 25 to 1,600 pg P4 or P5 / tube and 12.5 to 800 pg T / tube (final volume 500 µl).

2.11. Analytical methods

Glucose, fructosamine, HbA1c, total cholesterol, HDL-cholesterol, creatinine and albumin in serum and / or urine were determined by using commercial kits (Wiener Laboratories, Rosario, Argentina). The volume of urine was estimated gravimetrically. Sodium was measured by flame photometry. Glomerular filtration rate (GFR), estimated by creatinine clearance, urine flow rate (UFR), and fractional excretion of water (FEH_2O), glucose (FEglucose) and sodium ($FENa^+$) were calculated by conventional formulae. Proteins were measured with Coomasie brilliant blue G250 (Sedmak and Grossberg, 1977).

2.12. Statistics

Results were expressed as mean ± SEM of 5-6 observations. Statistics was performed using the one-way analysis of variance followed by t-Student or Newman Keuls test as adequate. A p-value ≤ 0.05 was considered as statistically significant.

3. Results

3.1. General conditions and serum biochemical parameters one week after STZ-induced diabetes

STZ-treated rats exhibited early stage diabetes characteristics. A significant decrease in the body weight (C= 351 ± 2, STZ= 302 ± 3 g, $p<0.01$) of the rats was observed one week after STZ injection compared to vehicle administration. Water intake (C= 5.4 ± 0.5, STZ= 9.2 ± 0.3 ml/d.100g, $p<0.05$) and urine flow rate (Table 1-B) were significantly higher in STZ group compared to C group. Glucose and lipid metabolism parameters are shown in Table 1-A. Serum glucose and fructosamine levels were augmented in STZ rats, while HbA1c concentration was not modified by the treatment, which is reasonable due to the short-term hyperglycemia. The lipid profile shows increased serum triglyceride values in rats treated with STZ, without changes in total cholesterol or HDL-cholesterol levels (Table 1-A).

3.2. Renal function one week after STZ-induced diabetes

Renal function studies showed that short-term treatment with STZ induces no changes in plasma creatinine levels or in glomerular filtration rate estimated as creatinine clearance. Tubular function parameters were significantly affected by diabetes induction. Urine flow rate and fractional excretions of water, glucose and sodium were higher in STZ-treated rats compared to controls. Urinary albumin excretion was not affected by the treatment. All these data are summarized in Table 1-B.

3.3. Renal histology one week after STZ-induced diabetes

In histological sections stained with hematoxylin-eosin (Fig. 1) and PAS (not shown), no morphological alterations were observed in the STZ kidneys compared to C group. Glomerular structure and the integrity of the brush border of cortical tubules were preserved in the STZ kidneys.

Masson's trichrome and Direct Red 80/picric acid stains were performed to assess fibrosis areas, which were not detected at this stage of induced-diabetes (not shown).

3.4. Kidney inflammation one week after STZ-induced diabetes

3.4.1. Inflammatory infiltrate

An interstitial inflammatory infiltrate, mainly in the outer medulla and in the cortex was found in STZ-treated animals. Inflammatory cell infiltration consists primarily of mononuclear cells with the presence of polymorphonuclear leukocytes (Fig. 1).

3.4.2. Myeloperoxidase activity

Myeloperoxidase activity was estimated as indicator of polymorphonuclear leukocytes infiltration. The enzyme activity was found to be increased in the kidneys of rats treated with STZ, both in cortical (C= 0.25 ± 0.07, STZ= 0.91 ± 0.25 O.D./min.g, $p<0.05$) and medullary (C= 0.22 ± 0.06, STZ= 0.74 ± 0.18 O.D./min.g, $p<0.05$) tissue.

3.4.3. Pro-inflammatory cytokines expression

IL-1β and IL-6 gene expression levels were increased in renal cortical and medullary tissue of rats treated with STZ compared to untreated animals. A similar pattern was found when IL-1β protein abundance was assessed by western blot. These results are presented in Fig. 2.

3.5. Renal expression of TGF-β mRNA one week after STZ-induced diabetes

PCR experiments indicated that STZ treatment increases mRNA expression of TGF-β in renal cortex. No significant changes were found in the expression of the messenger in medullary tissue (Fig. 3).

3.6. Renal expression of HSP70 protein one week after STZ-induced diabetes

Expression of HSP 70 was investigated to assess the renal response to stress induced by early diabetes. An increase in HSP70 expression was observed in both renal cortex and medulla of STZ rats compared to control group (Fig. 4).

3.7. Serum concentration and renal content of progesterone and testosterone one week after STZ-induced diabetes

P4 and T levels were determined by RIA. Results are presented in Table 2. It was observed that serum concentrations of P4 and T were significantly decreased (60% and 80%, respectively) in STZ group compared to C group. P4 content in renal medullary tissue decreased significantly in STZ-treated rats compared to untreated animals, while the decreasing trend in cortical tissue did not reach statistical significance. T renal content was found significantly decreased in the STZ group both at cortical and medullary levels.

3.8. Renal expression of TSPO, StAR and CYP11A1 one week after STZ-induced diabetes

TSPO mRNA expression was not significantly changed with STZ treatment in renal cortex or medulla (Fig. 5). Also, no changes were found in the levels of TSPO protein in cortical or medullary tissue (Fig.6).

A significant decrease in StAR mRNA expression was observed in kidney tissue of STZ rats compared to C group. A reduction of approximately 47% in cortical tissue and 70% in medullary tissue was observed (Fig. 5). StAR protein was detected in isolated mitochondria samples by Western blot. As shown in Fig. 6, STZ-treatment induced a significant decrease in medullary StAR protein expression. The 35% protein levels reduction found in cortical samples did not reach statistical significance.

CYP11A1 protein abundance was investigated by Western blot in IMM-enriched fractions. CYP11A1 protein expression was significantly decreased by STZ-treatment in both cortical (33%) and medullary (65%) samples (Fig. 6).

3.9. Immunohistochemical renal localization of StAR and CYP11A1 protein one week after STZ-induced diabetes

Immunostaining for StAR and CYP11A1 can be seen in Fig. 7 and 8, respectively. Both proteins showed similar immunohistochemical distribution pattern along the nephron in control kidneys, as previously reported by our group (Pagotto et al., 2011). Positive staining can be mainly observed in cortical distal convoluted tubules (StAR: Fig. 7- A and B; CYP11A1: Fig. 8- A and B) and in outer medullary thick ascending limb of Henle´s loop (StAR: Fig. 7- E and F; CYP11A1: Fig. 8- E and F). STZ-treatment did not change the distribution of these proteins in the renal structures, but immunostaining for StAR (Fig. 7- C and D; G and H) and CYP11A1 (Fig. 8- C and D; G and H) was markedly weaker compared to the respective controls.

3.10. Renal synthesis of Pregnenolone and Progesterone one week after STZ-induced diabetes

Pregnenolone and progesterone synthesis was evaluated in isolated mitochondria from renal cortex and medulla. Renal synthesis of these steroids in basal conditions was previously described by our group (Pagoto et al., 2011). The present study compares the responses to the addition of the membrane-permeable cholesterol analogue, 22R-OHC, between mitochondria isolated from control and STZ-treated rats (Fig. 9).

In the absence of 22R-OHC no difference in P5 synthesis rate was observed between C and STZ groups. In control samples, the presence of 22R-OHC induced a 5-fold increase in pregnenolone production at cortical level and a 60-fold increase at medullary level. STZ treatment did not change the rate of pregnenolone synthesis in cortical mitochondria, but caused a 95% reduction in medullary samples compared to the untreated group.

In the control group, the addition of 22R-OHC to the reaction buffer increased the rate of progesterone synthesis in medullary mitochondria, with no change in hormone production in the cortex samples. The increase in progesterone synthesis in medulla was found to be nullified in the STZ group.

4. Discussion

The main finding of this study is that an early stage of diabetes induces a decrease in renal expression of steroidogenic molecules and inhibits CYP11A1 function and the consequent local production of pregnenolone, the key precursor to the other steroid hormones. Studies from other laboratories have described the association between alteration in serum levels of sex hormones and decline of renal function in the progression of diabetes (Maric, 2009, Wang et al., 2019). The evidence found in this work, that diabetes also inhibits local

steroidogenesis, would provide a novel and broader approach to studies of steroid hormones in the pathophysiology of diabetic kidney disease.

A short-term diabetes model has been used in this study. After one week of STZ administration, animals presented characteristics of early diabetes, including hyperglycemia, polydipsia, polyuria and body weight loss. Analysis of the lipid profile showed that only plasma triglyceride levels are increased in these animals, indicating that the short-term hyperglycemia has not been able to severely alter the lipid metabolism, as occurs in advanced diabetes (Reaven E. and Reaven G., 1974; Newairy et al., 2002; Almeida et al., 2012). Renal studies showed that STZ treatment induces diuresis, natriuresis and glucosuria. These alterations in tubular function are consequence of hyperglycemia causing an osmotic diuresis (Liamis et al., 2014). At an early stage of experimental diabetes, we show that kidney histology, serum creatinine levels and glomerular filtration rate are still preserved, and urinary albumin excretion is not detected. These evidences indicate that it is a stage prior to renal decline, which occurs later after STZ injection (Krishan et al., 2017). Activation of an inflammatory process was found in renal tissue of these diabetic rats. Besides an interstitial leukocyte infiltrate, increased myeloperoxidase activity was detected, which would contribute to oxidative stress and corroborates not only the presence of the leukocyte infiltrate but also the activation of these cells (Maruyama et al., 2004; Ysebaert et al., 2000; Pompermayer et al., 2005). We also observed an increase in mRNA expression of the proinflammatory cytokines, IL-6 and IL-1β, in agreement with studies from other authors (Sassy-Prigent et al., 2000). In addition, an increase in protein expression of IL-1β in renal tissue of STZ groups was demonstrated. The expression of TGF-β1 mRNA was increased in cortical tissue of diabetic rats. The increase in TGF-β1 mRNA has been reported since 24 h up to 15 weeks after STZ administration in the cortex and particularly in the glomeruli, the main target of the TGF-β1 trophic actions; increased TGF-β1 abundance was detected 2 weeks after STZ treatment (Yamamoto et al., 1993; Shankland et al., 1994; Lane et al., 2001). HSP70 expression was found to be increased in the kidneys of these short-term diabetic rats, as was observed in rats from 4 weeks after administration of STZ (Barutta et al., 2008). Interestingly, other authors have described inhibition in steroidogenic activity associated with inflammation (Leisegang and Henkel, 2018; Slominski et al., 2013) or HSP70 expression (Liu and Stocco, 1997) in different experimental models. In turn, evidence indicates that the processes of steroidogenesis, inflammation and stress response might interact in a complex way (Khanna et al., 1995; Jheng et al., 2015; Chebotareva et al., 2017).

Therefore, at this early stage of diabetes the kidney does not yet show obvious signs of structural or functional impairment. However, some mechanisms involved in the onset and

progression of diabetic kidney disease have already been triggered, such as expression of mediators of inflammation, fibrosis, and stress response. In this scenario, renal steroidogenesis was evaluated.

In a series of experiments, we studied the expression of proteins associated with cholesterol transport to the IMM. The expression of TSPO neither at the messenger nor at the protein level changed with STZ-treatment compared to the controls. Nevertheless, the renal expression of StAR was significantly decreased in diabetic rats at the medullary level. This reduction in the abundance of StAR could affect, in some way, cholesterol transport. In our pregnenolone synthesis experiments in the absence of 22R-OHC, we found low P5 production rate, which other authors call the net synthesis of pregnenolone from endogenous cholesterol (Espinosa-García et al, 2000). In these experimental conditions, no difference was observed between control and STZ samples, although the expression of StAR is decreased in the STZ group. This finding suggests that StAR-independent mechanisms could be involved in cholesterol transport to IMM. StAR-independent mechanisms have been proposed in steroidogenic and non-steroidogenic cells (Miller and Gucev, 2014). Cholesterol that reaches the inner mitochondrial membrane is a substrate for the CYP11A1, the rate-limiting enzyme of steroidogenesis, which catalyzes the conversion of cholesterol to pregnenolone. In a previous work from our laboratory, we demonstrated that CYP11A1 localized in rat renal tissue actually corresponds to an active form of the enzyme (Pagotto et al., 2011). In the present experiments, it was found that the expression of CYP11A1 was significantly decreased in diabetic rats, which could affect renal steroidogenesis. To assess the key enzyme CYP11A1 function, the rate of pregnenolone synthesis in the presence of 22R-OHC was evaluated in mitochondria isolated from the cortex and medulla of diabetic and control rats. STZ treatment significantly decreased the rate of pregnenolone synthesis, this decrease being more pronounced at the medulla level, approximately 95% compared to untreated group. The important finding of this work is the decrease in renal steroidogenesis in STZ-treated rats. Previously, we demonstrated that the steroidogenic machinery in basal conditions is mainly activated at the medullary level, suggesting that in this region the paracrine/autocrine action of steroids would be essential (Pagotto et al., 2011). Although such steroid actions have not yet been elucidated, the presence of the complete active storiodogenic machinery in kidney tissue strongly indicates that the local synthesis of steroid hormones would have significant biological implication. In this work, we demonstrated that STZ treatment reduces steroidogenic proteins expression and pregnenolone synthesis to a greater extent precisely in the medulla, suggesting that diabetes might impair nephrosteroids-dependent mechanisms. Pregnenolone may be converted to dehydroepiandrosterone by CYP17A1 (Cytochrome

P450c17), to pregnenolone sulfate by steroid sulfotransferase and to progesterone by 3β-hydroxysteroid dehydrogenase (3β-HSD) in rat kidney tissue (Dalla Valle et al., 1992 and 2004; Kohjitani et al., 2006). Some indirect evidence may lead to hypothesize that the decrease in pregnenolone would be harmful to the kidney. In this sense, pregnenolone and its metabolites have been reported to exert protective effects, by modulating $GABA_A$ receptors, on renal epithelial cells undergoing mitochondrial inhibition (Waters et al., 1997). The possible role of the $GABA_A$ receptor in the local regulation of kidney function was previously proposed by our group (Monasterolo et al., 1996). Recently, decreased pregnenolone sulfate has been proposed as a biomarker in the detection of end-stage kidney disease (Boelaert et al., 2017), reaffirming the implication of this steroid hormone in renal pathophysiology, and stimulating research on both its actions and its processing in the kidney.

We found a significant decrease in progesterone production in medullary mitochondria of diabetic rats. This fact could be a consequence of the significant decrease in pregnenolone synthesis, although alterations in the expression and / or activity of 3β-HSD should not be ruled out. Tissue steroid content depends on uptake of circulating steroids and on local biosynthesis. In this study, the measured levels of steroid hormones were markedly higher in renal tissue than in systemic circulation, which can be considered as evidence in favor of local steroidogenesis. Plasma progesterone concentration was significantly decreased in diabetic rats. However, the reduction of the progesterone content in kidney tissue was only observed in the medulla, in coincidence with the decreased progesterone production observed "*in vitro*" in medullary mitochondria of STZ-treated rats. These results reinforce the idea that local steroidogenesis would significantly contribute to renal progesterone content. The decrease in the renal bioavailability of progesterone that is already observed in this early stage of diabetes could contribute to activation of damaging mechanisms. This speculation is based on the fact that progesterone replacement improves functional and structural disturbances in experimental models of diabetic nephropathy in rats (Al-trad et al., 2015). Advanced stage of experimental diabetes has been reported to cause other disturbances in the renal steroidogenic pathway, such as increased aromatase activity associated with enhanced tissue estrogen content and augmented expression of estrogen receptor alpha protein (Prabhu et al., 2010). Aromatase inhibitor treatment attenuated diabetes-induced kidney damage (Manigrasso et al., 2011). Taken together, all this evidence indicates that alterations of different steps in the renal steroidogenic pathway take place since the onset of diabetes and seem to accompany its progression. Nevertheless, knowing the precise role of nephrosteroids

in renal physiology and in the development of kidney damage associated with diabetes requires further investigation.

Experimental diabetes also inhibits steroidogenesis in the central nervous system, where it has been proposed that the decrease in neurosteroids would be detrimental (Romano et al., 2017 and 2018; Murugan et al., 2019). This evidence and our results together suggest that the diabetic state alters steroid biosynthesis in different non-classical steroidogenic tissues, triggering mechanisms with potential relevance for the integrity of these target organs.

Conclusion:

This study shows that a very early stage of diabetes induces the inhibition of renal steroidogenic capacity, especially in CY11A1 function, with the consequent decrease in the production of pregnenolone, the precursor of all steroid hormones. This deterioration in steroid synthesis takes place in an environment of inflammation and increased expression of HSP70, factors that could be modulating the steroidogenic process. Elucidation of both the role of nephrosteroids and the possible interrelationship between local steroidogenesis, inflammatory process, and HSP70 signaling pathways could expand our knowledge of the pathophysiology of diabetic kidney disease and expose innovative pharmacological targets.

Funding

This work was supported by National Scientific and Technical Research Council (CONICET) (Grant PIP0309 to LAM) and National University of Rosario (Grant BIO508 to LAM).

Acknowledgements

We are thankful to Dr. Walter L. Miller and Dr. Dale B. Hales for kindly supplying us with the anti-StAR and anti- CYP11A1 antibodies, respectively. We also thank Wiener Laboratories, Rosario, Argentina, for the gift of analytical reagents.

Declarations of interest

None

References

Almeida, D., Pereira Braga, C., Lourenzi Barbosa Novelli , E., Henrique Fernandes, A., 2012. Evaluation of Lipid Profile and Oxidative Stress in STZ Induced Rats Treated with

Antioxidant Vitamin. Braz. Arch. Biol. Technol. 55, 527-536. https://doi.org/10.1590/S1516-89132012000400007

Al-Trad, B., Ashankyty, I., Alaraj, M., 2015. Progesterone ameliorates diabetic nephropathy in streptozotocin-induced diabetic Rats. Diabetol. Metab. Syndr. 7, 97-109. https://doi.org/10.1186/s13098-015-0097-1

Barutta, F., Pinach, S., Giunti, S., Vittone, F., Forbes, J., Chiarle, R., Arnstein, M., Cavallo Perin, C., Camussi, G., Cooper, M., Gruden, G., 2008. Heat shock protein expression in diabetic nephropathy. Am. J. Physiol. Renal Physiol. 295, F1817–F1824. https://doi.org/10.1152/ajprenal.90234.2008

Boelaert, J., Lynen, F., Glorieux, G., Schepers, E., Neirynck, N., Vanholder, R., 2017. Metabolic profiling of human plasma and urine in chronic kidney disease by hydrophilic interaction liquid chromatography coupled with time-of-flight mass spectrometry: a pilot study. Anal. Bioanal. Chem. 409, 2201-2211. https://doi.org/10.1007/s00216-016-0165-x.

Brovedan, M., Molinas, S., Pisani, G., Monasterolo, L., Trumper, L., 2017. Glutamine protection in an experimental model of acetaminophen nephrotoxicity. Can. J. Physiol. Pharmacol. 96: 366–371. https://doi.org/10.1139/cjpp-2017-0423

Calamita, G., Ferri, D., Gena, P., Liquori, G., Cavalier, A., Thomas, D., Svelto, M., 2005. The inner mitochondrial membrane has aquaporin-8 water channels and is highly permeable to water. J. Biol. Chem. 280, 17149-17153. https://doi.org/10.1074/jbc.C400595200

Chebotareva, N., Bobkova1, I., Shilov, E., 2017. Heat shock proteins and kidney disease: perspectives of HSP Therapy. Cell Stress and Chaperones 22, 319–343. https://doi.org/10.1007/s12192-017-0790-0

DallaValle, L., Belvedere, P., Simontacchi, C., Colombo, L., 1992. Extraglandular hormonal steroidogenesis in aged rats. J. Steroid Biochem. Mol. Biol. 43, 1095-1098. https://doi.org/10.1016/0960-0760(92)90337-I

Dalla Valle, L., Toffolo, V., Vianello, S., Belvedere, P., Colombo, L., 2004. Expression of cytochrome P450c17 and other steroid-converting enzymes in the rat kidney throughout the

life-span. J. Steroid Biochem. Mol. Biol. 91:49-58. https://doi.org/10.1016/j.jsbmb.2004.01.008

Espinosa-Garcia, M, Strauss, J., Martinez, F., 2000. A trypsin-sensitive protein is required for utilization of exogenous cholesterol for pregnenolone synthesis by placental mitochondria. Placenta 21, 654-660. https://doi.org/10.1053/plac.2000.0562

Esparza-Perusquía, M., Olvera-Sánchez, S., Flores-Herrera, O., Flores-Herrera, H., Guevara-Flores, A., Pardo, J., Espinosa-García, M., Martínez, F., 2015. Mitochondrial proteases act on STARD3 to activate progesterone synthesis in human syncytiotrophoblast. Biochim. Biophys. Acta 1850: 107-117. http://dx.doi.org/10.1016/j.bbagen.2014.10.009

Farkash, Y., Timberg, R., Orly, J., 1986. Preparation of antiserum to rat cytochrome P-450 cholesterol side chain cleavage, and its use for ultrastructural localization of the immunoreactive enzyme by protein A-gold technique. Endocrinology 118, 1353–1365. https://doi.org/10.1210/endo-118-4-1353

Jheng, H-F., Tsai, P-J., Chuang, Y-L., Shen, Y-T., Tai, T-A., Chen, W-C., Chou, C-K., Ho, L-C., Tang, M-J., Lai, K-T., Sung, J-M., Tsai, Y-S., 2015. Albumin stimulates renal tubular inflammation through an HSP70-TLR4 axis in mice with early diabetic nephropathy Dis. Model. Mech. 8, 1311-1321. https://doi.org/10.1242/dmm.019398

Khanna, A., Aten, R., Behrman, H., 1995. Physiological and pharmacological Inhibitors of Luteinizing Hormone-Dependent Steroidogenesis Induce Heat Shock Protein-70 in Rat Luteal Cells. Endocrinology 136, 1775-1781. https://doi.org/10.1210/endo.136.4.7895690

Kohjitani, A., Fuda, H., Hanyu, O., Strott, C., 2006. Cloning, characterization and tissue expression of rat SULT2B1a and SULT2B1b steroid/sterol sulfotransferase isoforms: Divergence of the rat SULT2B1 gene structure from orthologous human and mouse genes. Gene 367, 66-73. https://doi.org/10.1016/j.gene.2005.09.009

Krishan, P., Singh, G., Bedi, O., 2017. Carbohydrate restriction ameliorates nephropathy by reducing oxidative stress and upregulating HIF-1α levels in type-1 diabetic rats J. Diabetes Metab. Disord. 16, 47-56. https://doi.org/10.1186/s40200-017-0331-5

Krueger, K., Papadopoulos, V., 1990. Peripheral-type Benzodiazepine Receptors Mediate Translocation of Cholesterol from Outer to Inner Mitochondrial Membranes in Adrenocortical Cells. J. Biol. Chem. 265, 15015-15022.

Krueger, R., Orme-Johnson, N., 1983. Acute adrenocorticotropic hormone stimulation of adrenal corticosteroidogenesis. J. Biol. Chem. 258,10159–10167.

Lane, P.H., Snelling, D.M., Langer, W.J., 2001. Streptozocin diabetes elevates all isoforms of TGF-beta in the rat kidney. Int. J. Exp. Diab. Res. 2, 55-62. https://doi.org/10.1155/EDR.2001.55

Leisegang, K., Henkel, R., 2018. The in vitro modulation of steroidogenesis by inflammatory cytokines and insulin in TM3 Leydig cells. Reprod. Biol. Endocrinol. 16, 26-36. https://doi.org/10.1186/s12958-018-0341-2

Liamis, G., Liberopoulos, E., Barkas, F., Elisaf, M., 2014. Diabetes mellitus and electrolyte disorders. World. J. Clin. Cases 16, 488-496. https://doi.org/10.12998/wjcc.v2.i10.488

Lin, D. , Sugawara, T., Strauss, J.III, Clark, B., Stocco, D., Saenger, P., Rogol, A., Miller. W., 1995. Role of steroidogenic acute regulatory protein in adrenal and gonadal steroidogenesis. Science 267, 1828–1831. https://doi.org/10.1126/science.7892608

Liu, Z., Stocco, D., 1997. Heat Shock-Induced Inhibition of Acute Steroidogenesis in MA-10 Cells Is Associated with Inhibition of the Synthesis of the Steroidogenic Acute Regulatory Protein. Endocrinology 7, 2722-2728. https://doi.org/10.1210/endo.138.7.5278

Manigrasso, M., Sawyer, R., Marbury, D., Flynn, E., Maric, C., 2011. Inhibition of estradiol synthesis attenuates renal injury in male streptozotocin (STZ)-induced diabetic rats. Am J. Physiol. Renal Physiol. 301:F634–F640. https://doi.org/10.1152/ajprenal.00718.2010

Maric, C., 2009. Sex, diabetes and the kidney. Am J Physiol Renal Physiol. 296, F680–F688. https://doi.org/10.1152/ajprenal.90505.2008

Maruyama, Y., Lindholm, B., Stenvinkel, P., 2004. Inflammation and oxidative stress in ESRD--the role of myeloperoxidase. J. Nephrol. 17, S72-6. PMID: 15599890

Miller, W., Gucev, Z., 2014. Disorders in the Initial Steps in Steroidogenesis, in: New, M., Lekarev, O., Parsa, A., Yuen, T., O´Malley, B., Hammer, G. (Eds.), Genetic Steroid Disorders. Elsevier Inc., pp. 145-164. http://dx.doi.org/10.1016/B978-0-12-416006-4.00011-9

Monasterolo, L., Trumper, L., Elías, M., 1996. Effects of Gamma-Aminobutyric Acid Agonists on the Isolated Perfused Rat Kidney. J. Pharmacol. Exp. Ther. 279, 602-607. PMID: 8930162

Murugan,S., Jakka, P., Namani, S., Mujumdar, V., Radhakrishnan, G., 2019. The neurosteroid pregnenolone promotes degradation of key proteins in the innate immune signaling to suppress inflammation. J. Biol. Chem. 294 , 4596–4607. https://doi.org/10.1074/jbc.RA118.005543

Newairy, A-S., Mansour, H., Yousef, M., Sheweita, S., 2002. Alterations of lipid profile in plasma and liver of diabetic rats: effect of hypoglycemic herbs. J. Environ. Sci. Health 37, 475-484. https://doi.org/10.1081/PFC-120014877

Nijtmans, L., de Jong, L., Artal Sanz, M., Coates, P., Berden, J., Back, J., Muijsers, A., van der Spek, H., Grivell, L., 2000. Prohibitins act as a membrane-bound chaperone for stabilization of mitocondrial proteins. EMBO J. 19, 2444-2451. https://doi.org/10.1093/emboj/19.11.2444

Pagotto, M., Roldán, M., Pagotto, R., Lugano, M., Pisani, G., Rogic, G., Molinas, S., Trumper, L., Pignataro, O., Monasterolo, L., 2011. Localization and functional activity of cytochrome P450 side chain cleavage enzyme (CYP11A1) in the adult rat kidney. Mol. Cell. Endocrinol. 30, 253-260. https://doi.org/10.1016/j.mce.2010.10.020

Papadopoulos, V., Miller, W., 2012. Role of mitochondria in steroidogenesis. Best. Pract. Res. Clin. Endocrinol. Metab. 26, 771–790. https://doi.org/10.1016/j.beem.2012.05.002

Pompermayer, K., Souza, D., Lara, G., Silveira, K., Cassali, G., Andrade, A., Bonjardim, C., Passaglio, K., Assreuy, J., Cunha, F., Vieira, M., Teixeira, M., 2005. The ATP-sensitive potassium channel blocker glibenclamide prevents renal ischemia/reperfusion injury in rats. Kidney Int. 67, 1785-1796. https://doi.org/10.1111/j.1523-1755.2005.00276.x

Prabhu, A., Xu, Q., Manigrasso, M., Biswas, M., Flynn, E., lliescu, R., Lephart, E., Maric, C., 2010. Expression of aromatase, androgen and estrogen receptors in peripheral target tissues in diabetes. Steroids 75, 779–787. https://doi.org/10.1016/j.steroids.2009.12.012

Reaven, E., Reaven, G., 1974. Mechanisms for development of diabetic hypertriglyceridemia in streptozotocin-treated rats. Effect of diet and duration of insulin deficiency. J Clin Invest 54:1167-1178. https://doi.org/10.1172/JCI107860

Romano, S., Mitro, N., Diviccaro, S., Spezzano, R., Audano, M., Garcia-Segura, L., Caruso, D., Cosimo Melcangi, R., 2017. Short-term effects of diabetes on neurosteroidogenesis in the rat hippocampus. J. Steroid Biochem. Mol. Biol. 167, 135–143. https://doi.org/10.1016/j.jsbmb.2016.11.019

Romano, S., Mitro, N., Giatti, S., Diviccaro, S., Pesaresi, M., Spezzano, G., Audano, M., Garcia-Segura, L., Donatella Caruso, Cosimo Melcangi, R., 2018. Diabetes induces mitochondrial dysfunction and alters cholesterol homeostasis and neurosteroidogenesis in the rat cerebral cortex. J. Steroid Biochem. Mol. Biol. 178, 108–116. https://doi.org/10.1016/j.jsbmb.2017.11.009

Sassy-Prigent, C., Heudes, D., Mandet, C., Belair, M.F., Michel, O., Perdereau, B., Bariety, J., Bruneval, P., 2000. Early glomerular macrophage recruitment in streptozotocin-induced diabetic rats. Diabetes 49, 466-475. https://doi.org/10.2337/diabetes.49.3.466

Schierwagen, C., Bylund-Fellenius, A.C., and Lundberg, C., 1990. Improved method for quantification of tissue PMN accumulation measured by myeloperoxidase activity. J. Pharmacol. Methods 23, 179–186. https://doi.org/10.1016/0160-5402(90)90061-o

Sedmak, J.J., Grossberg, S.E., 1977. A rapid, sensitive, and versatile assay for protein using Coomassie brilliant blue G250. Anal. Biochem. 79, 544–552. https://doi.org/10.1016/0003-2697(77)90428-6

Shankland, S., Scholey, J., Ly, H., Thai, K., 1994. Expression of transforming growth factor-beta 1 during diabetic renal hypertrophy. Kidney Int. 46, 430-442. htts://doi.org/10.1038/ki.1994.291.

Slominski, A., Zbytek, B., Nikolakis, G., Manna, P., Skobowiat, C., Zmijewski, M., Li, W., Janjetovic, Z., Postlethwaite, A., Zouboulis, C., Tuckey, R., 2013. Steroidogenesis in the skin: implications for local immune functions. J. Steroid Biochem. Mol. Biol. 137, 107–123. https://doi.org/10.1016/j.jsbmb.2013.02.006

Stocco, D., Zhao, A., Tu, L., Morohaku, K., Selvaraj, V., 2017. A brief history of the search for the protein(s) involved in the acute regulation of steroidogenesis. Mol. Cell. Endocrinol. 441, 7–16. https://doi.org/10.1016/j.mce.2016.07.036

Sulaiman, M.K. 2019. Diabetic nephropathy: recent advances in pathophysiology and challenges in dietary management. Diabetol. Metab. Syndr. 11, 7-11. https://doi.org/10.1186/s13098-019-0403-4

Wang, C., Zhang, W., Wang, Y., Wan, H., Chen, Y., Xia, F., Zhang, K., Wang, N., Lu, Y., 2019. Novel associations between sex hormones and diabetic vascular complications in men and postmenopausal women: a cross−sectional study. Cardiovasc. Diabetol. 18, 97-107. https://doi.org/10.1186/s12933-019-0901-6

Waters, S., Miller, G.W., Aleo, M., Schnellmann, R., 1997. Neurosteroid inhibition of cell death. Am. J. Physiol. Renal Physiol. 273, 869-876. https://doi.org/10.1152/ajprenal.1997.273.6.F869

Xu, Q., Wells, C.C., Garman, J.H., Asico, L., Escano, C.S., Maric, C., 2008. Imbalance in sex hormone levels exacerbates diabetic renal disease. Hypertension 51, 1218-1224. https://doi.org/10.1161/HYPERTENSIONAHA.107.100594

Xu, Q., Prabhu, A., Xu, S., Manigrasso, M.B., Maric, C., 2009. Dose-dependent effects of dihydrotestosterone in the streptozotocin-induced diabetic rat kidney. Am. J. Physiol. Renal Physiol. 297, F307-315. https://doi.org/10.1152/ajprenal.00135.2009

Yamamoto, T., Nakamura, T., Noble, N.A., Ruoslahti, E., Border, W.A., 1993. Expression of transforming growth factor beta is elevated in human and experimental diabetic nephropathy. Proc. Natl. Acad. Sci. USA 90, 1814-1818. https://doi.org/10.1073/pnas.90.5.1814

Ysebaert, D.K., De Greef, K.E., Vercauteren, S.R., Ghielli, M., Verpooten, G.A., Eyskens, E.J., De Broe, M.E., 2000. Identification and kinetics of leukocytes after severe ischaemia/reperfusion renal injury. Nephrol. Dial. Transplant. 15:1562-1574. https://doi.org/10.1093/ndt/15.10.1562

Ziyadeh, F.N., 2004. Mediators of diabetic renal disease: the case for TGF-Beta as the major mediator. J. Am. Soc Nephrol. 1, S55-57. https://doi.org/10.1097/01.asn.0000093460.24823.5b

Table 1: (A) Glucose and lipid metabolism parameters and (B) renal function parameters in control and STZ-treated rats.

		Control	STZ
A	Plasma glucose (g/l)	0.82 ± 0.05	3.50 ± 0.75 *
	Plasma fructosamine (mmol/l)	1.25 ± 0.21	2.17 ± 0.06 *
	Plasma HbA1c (%)	3.82 ± 0.19	4.10 ± 0.13
	Plasma total cholesterol (mg/dl)	68 ± 2	63 ± 14
	Plasma triglyceride (mg/dl)	53 ± 5	106 ± 22*
	Plasma HDL-cholesterol (mg/dl)	23 ± 1	22 ± 1
	Plasma LDL-cholesterol (mg/dl)	34 ± 5	26 ± 4
B	Plasma creatinine (mg/dl)	0.62 ± 0.08	0.73 ± 0.07
	Creatinine clearance (µl/min.g)	410 ± 50	338 ± 55
	Urine flow rate (µl/min.g)	5.0 ± 0.2	8.7 ± 0.6 *
	FE H_2O (%)	1.33 ± 0.08	2.16 ± 0.32 *
	FE glucose(%)	0.016 ± 0.002	3.723 ± 1.016 *
	FE Na^+ (%)	0.33 ± 0.07	0.83 ± 0.15 *
	mg albumin/mg Creatinine	0.42 ± 0.17	0.44 ± 0.11

Measurements were performed one week after STZ or vehicle administration. Values represent means ± SEM. Results were obtained from 6 rats per group. * $p < 0.05$ *vs* C.

Table 2: Serum and renal content of Progesterone and Testosterone in control and STZ-treated rats.

		Control	STZ
Progesterone	Serum (pg/ml)	4.02 ± 1.32	1.65 ± 0.54 *
	Renal cortex (pg/mg tissue)	13.7 ± 2.6	11.0 ± 1.2
	Renal medulla (pg/mg tissue)	28.7 ± 4.7	2.9 ± 1.8 *
Testosterone	Serum (ng/ml)	1.15 ± 0.35	0.20 ± 0.04 *
	Renal cortex (ng/mg tissue)	2.9 ± 0.6	0.58 ± 0.2 *
	Renal medulla (ng/mg tissue)	4.3 ± 1.1	0.62 ± 0.4 *

Values represent means ± SEM. Results were obtained from 6 rats per group. * $p < 0.05$ *vs* C.

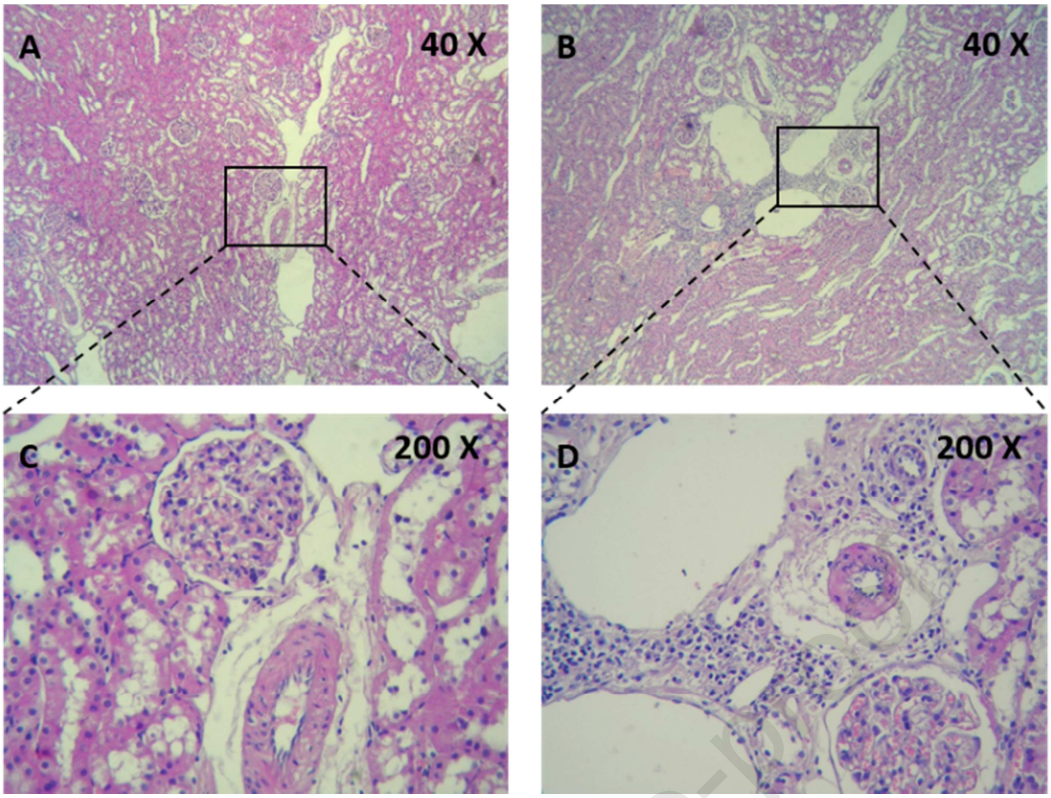

Figure 1: Photographs of histological sections of kidneys stained with H&E. No morphological changes were observed regarding the corpuscular, tubular or vascular structures in STZ section (B) compared to control (A). In the lower panel, a higher-magnification view shows an interstitial inflammatory infiltrate in the perivascular areas of the diabetic kidney (D). The infiltrate is not observed in control preparation (C). Magnification is indicated in each photo.

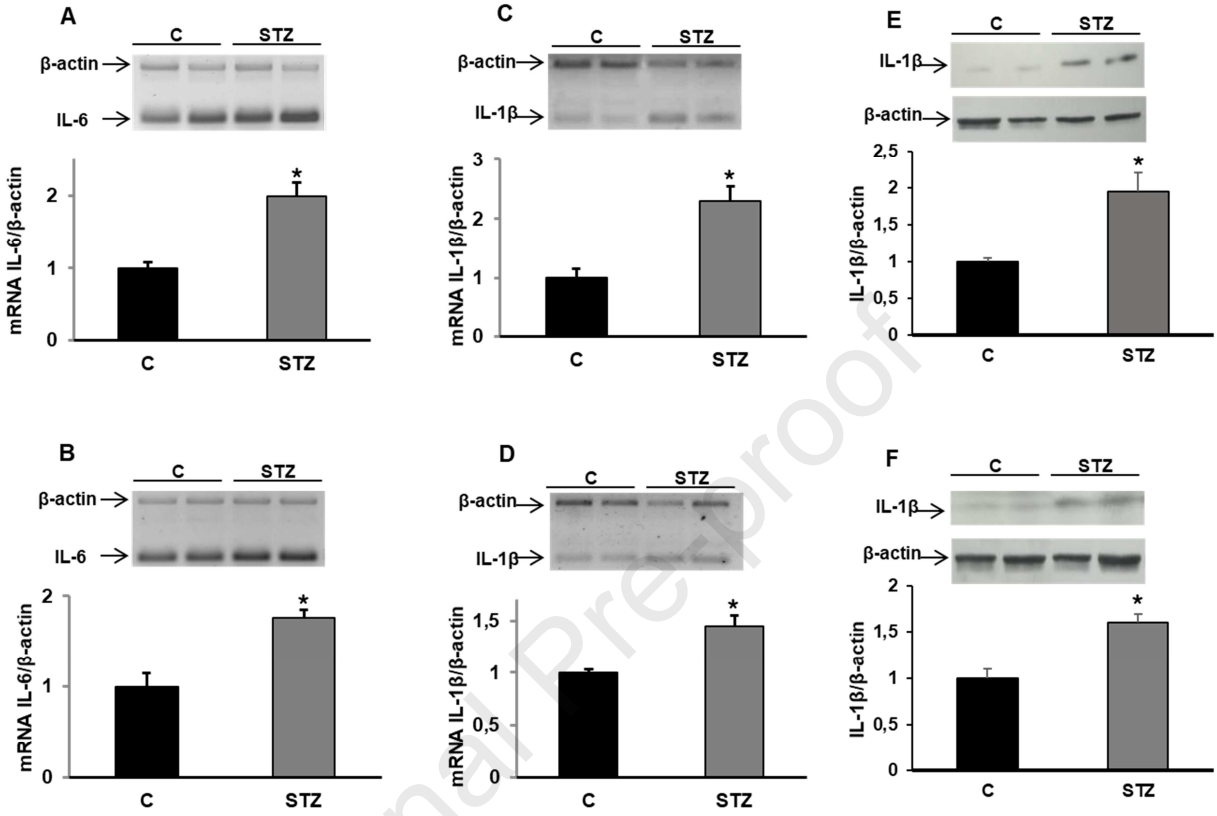

Figure 2: Renal expression of pro-inflammatory cytokines at an early stage of STZ-induced diabetes.

Representative gel images show mRNA levels of IL-6 (A, B) and IL-1β (C, D) in cortical (A, C) and medullary (B, D) renal tissue obtained from control and STZ-treated rats. Representative western blot images show the protein levels of IL-1β in cortical (E) and medullary (F) renal tissue obtained from control and STZ-treated rats. Bars represent mean ± SEM of 6 observations per group. * $p < 0.05$ *vs* C.

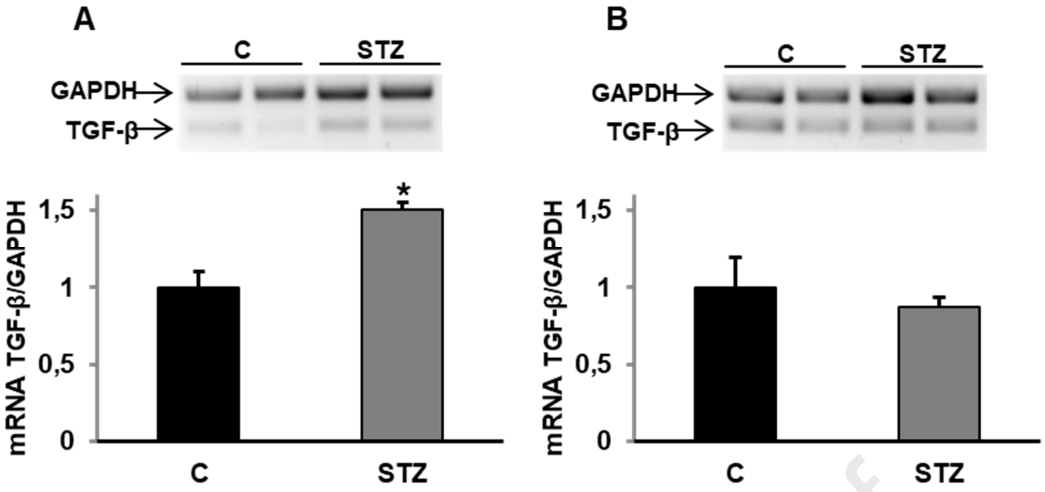

Figure 3: Renal expression of TGF-β1 mRNA at an early stage of STZ-induced diabetes. Representative gel images show mRNA levels of TGF-β1 in cortical (A) and medullary (B) renal tissue obtained from control and STZ-treated rats. Bars represent mean ± SEM of 6 observations per group. * $p < 0.05$ *vs* C.

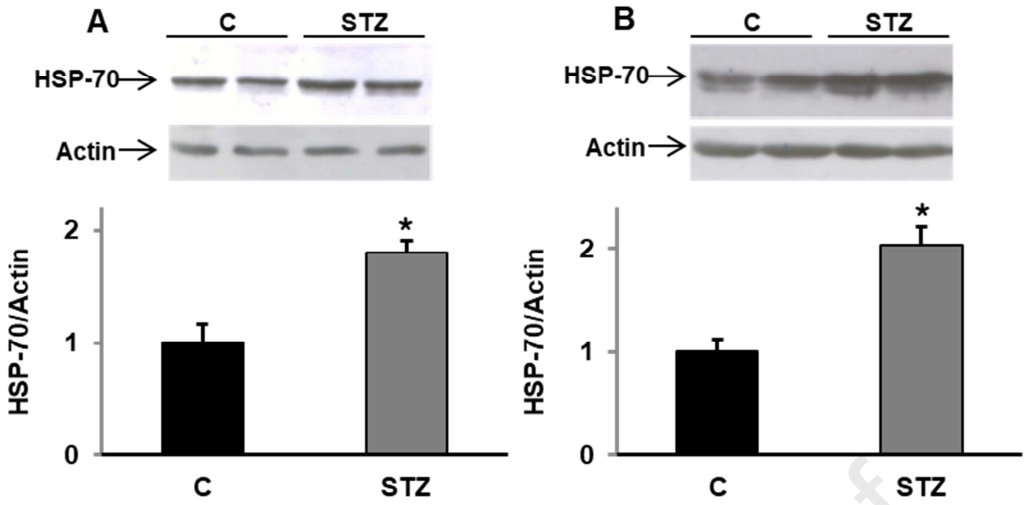

Figure 4: Renal expression of HSP-70 at an early stage of STZ-induced diabetes.

Representative western blot images show the protein levels of HSP70 in cortical (A) and medullary (B) renal tissue obtained from control and STZ-treated rats. Bars represent mean ± SEM of 6 observations per group. * $p < 0.05$ *vs* C.

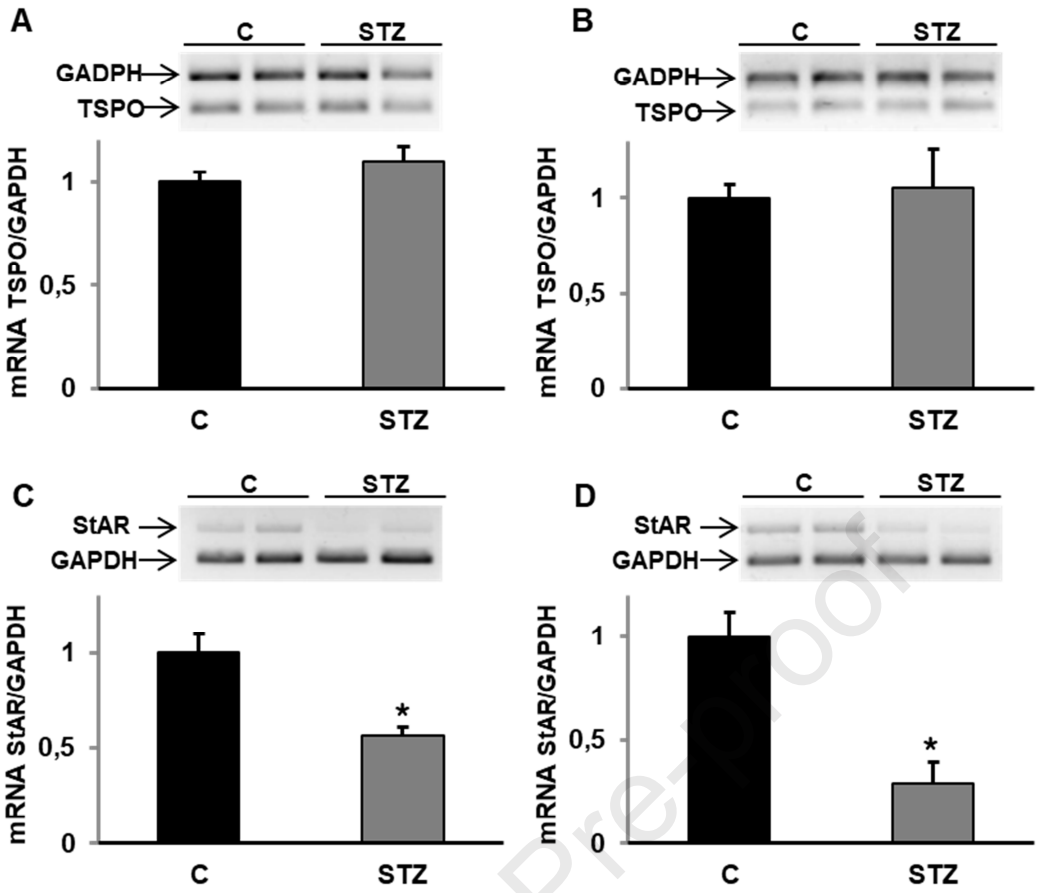

Figure 5: Renal mRNA expression of TSPO and StAR at early stage of STZ-induced diabetes. Representative gel images show mRNA levels of TSPO (A, B) and StAR (C, D) in cortical (A, C) and medullar (B, D) renal tissue obtained from control and STZ-treated rats. Bars represent mean ± SEM of 6 observations per group. * $p < 0.05$ *vs* C.

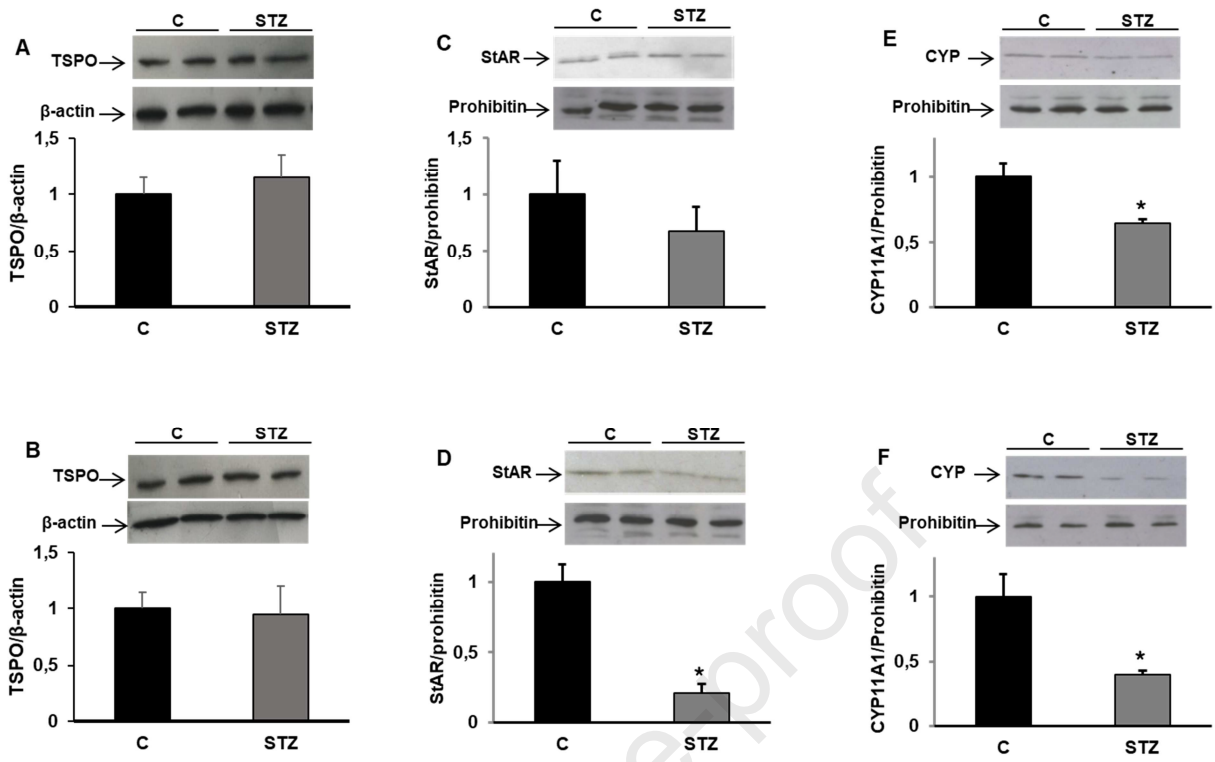

Figure 6: Renal expression of TSPO, StAR and CYP11A1 at early stage of STZ-induced diabetes. Representative western blot images of protein levels of: TSPO in cortical (A) and medullary (B) kidney tissue samples; StAR in cortical (C) and medullary (D) mitochondrial samples and CYP11A1 in cortical (E) and medullary (F) inner membrane mitochondrial samples obtained from control and STZ-treated rats. Bars represent mean ± SEM of 6 observations per group. * $p < 0.05$ *vs* C.

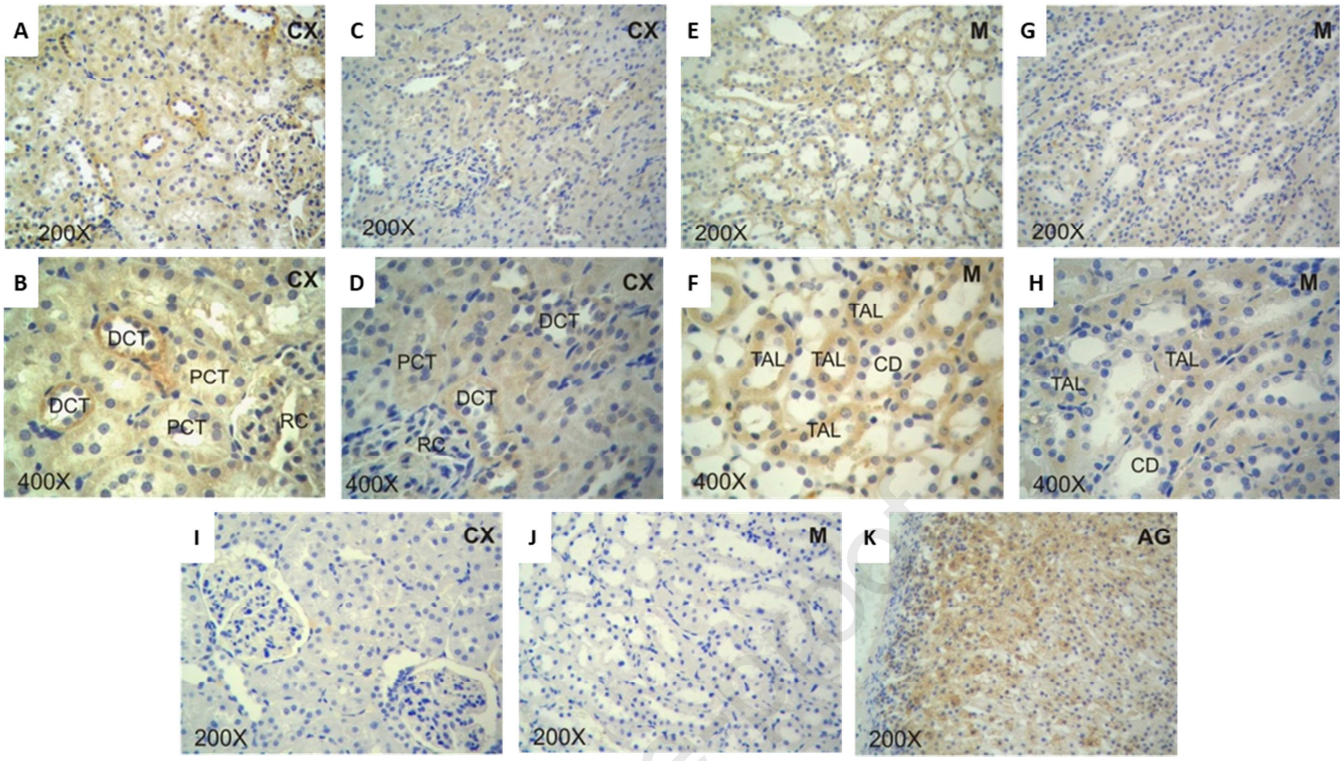

Figure 7: Immunohistochemical expression of StAR in kidney tissue of control (A, B, E and F) and STZ-treated (C, D, G and H) rats. The slices were incubated with anti-StAR antibody. The distal convoluted tubule (DCT) in the renal cortex (C and D) and the thick ascending limb of Henle's loop (TAL) in the external medulla (G and H) of STZ-treated rats presented lower staining intensity with respect to controls (A, B and E, F, respectively). Cortical (I) and medullary (J) sections were incubated in the presence of rabbit serum to replace the primary antibody and no positive mark was obtained. The specificity of the anti-StAR antibody was corroborated using sections of the adrenal gland (AG), observing a positive immune mark (K). CD: collecting duct, RC: renal corpuscle, PCT: proximal convoluted tubule, CX: renal cortex, M: renal medulla.

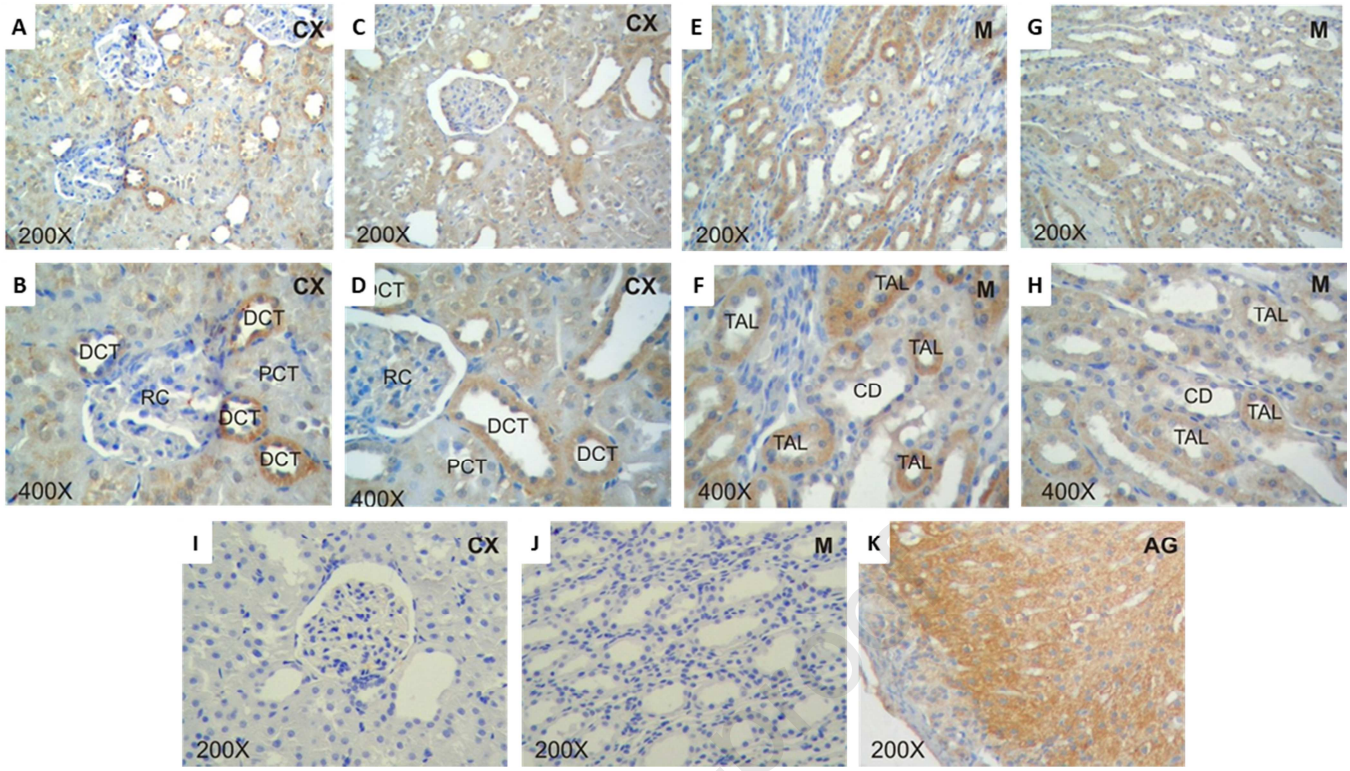

Figure 8: Immunohistochemical expression of CYP11A1 in kidney tissue of control (A, B, E and F) and STZ-treated (C, D, G and H) rats. The sections were incubated in the presence of anti-CYP11A1 antibody. Dimmer marking was observed in diabetic rat preparations, especially in the distal convoluted tubule (DCT) in the cortex (C and D) and in tubules of the thick ascending limb of Henle's loop (TAL) in the external medulla (G and H) with respect to the controls (A, B and E, F, respectively). Cortical (I) and medullary (J) sections were incubated with rabbit serum to replace the primary antibody, without obtaining a positive label. The specificity of the anti-CYP11A1 antibody was corroborated using sections of the adrenal gland (AG), showing a positive immune mark (K). CD: collecting duct, RC: renal corpuscle, PCT: proximal convoluted tubule, CX: renal cortex, M: renal medulla.

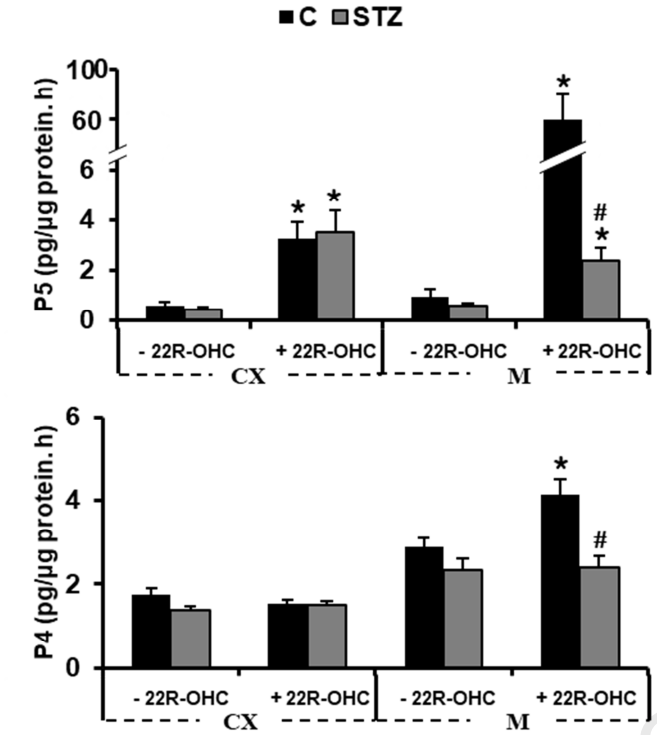

Figure 9: Renal synthesis of pregnenolone (P5) and progesterone (P4) at an early stage of diabetes. Isolated mitochondria from renal cortex (CX) and medulla (M) were incubated in reaction buffer in the presence (+22R-OHC) or absence (-22R-OHC) of 22R-hydroxycholesterol for 45 min. P5 and P4 were measured by RIA. Bars represent mean ± SEM of 6 observations per group. * $p < 0.05$ *vs* corresponding group in the absence of 22R-OHC. # $p<0.05$ *vs* control.

Highlights

1. Early diabetes inhibits renal synthesis of pregnenolone and progesterone
2. Medullary CYP11A1 expression and function are suppressed by STZ-induced diabetes
3. Steroidogenesis inhibition occurs prior to functional and structural changes
4. Decreased steroidogenesis is associated with inflammation and stress response

CRediT author statement:

Melina A. Pagotto: Conceptualization, Investigation, Writing- Original draft preparation. **María L. Roldán:** Investigation. **Sara M. Molinas:** Investigation, Writing - Review & Editing. **Trinidad Raices:** Investigation, Writing - Review & Editing. **Gerardo B. Pisani:** Investigation. **Omar P. Pignataro:** Conceptualization, Supervision. **Liliana A. Monasterolo:** Conceptualization, Writing- Original draft preparation, Funding acquisition, Supervision.

Highlights

1. Early diabetes inhibits renal synthesis of pregnenolone and progesterone
2. Medullary CYP11A1 expression and function are suppressed by STZ-induced diabetes
3. Steroidogenesis inhibition occurs prior to functional and structural changes
4. Decreased steroidogenesis is associated with inflammation and stress response